Chemical Engineering Journal 98 (2004) 165–173

Chemical Engineering Journal

www.elsevier.com/locate/cej

Investigations on the column performance of fluoride adsorption by activated alumina in a fixed-bed

Subhashini Ghorai, K.K. Pant*

Department of Chemical Engineering, Indian Institute of Technology, New Delhi 110016, India

Accepted 2 July 2003

Abstract

In the present study, removal of fluoride ions using activated alumina (AA) was investigated in batch and continuous operations. The fluoride removal performance was investigated as a function of the fluoride concentration, flow rate, amount of adsorbent dose and pH. Sorption data have been correlated with Langmuir and Freundlich isotherms. pH was shown to be a decisive parameter on fluoride removal. Percentage fluoride removal as a function of time and uptake capacity related to flow volume were determined by evaluating the breakthrough curves.

Data confirmed that early saturation and lower fluoride removal was observed at higher flow rate and at higher concentration. There was a marginal decrease in the uptake capacity after each regeneration cycle. A one-dimensional model for isothermal, axially dispersed fixed-bed adsorption has been numerically solved and compared with the experimental results. Predicted simulation results based on the assumption of pore-diffusion rate-control conditions matches with the experimental data in the initial zone of the breakthrough curve, but deviated marginally in the final tailing zone.

Keywords: Fluoride; Activated alumina; Regeneration; Drinking water; Breakthrough; Modeling

1. Introduction

Fluorine is present, as F^- in natural waters, and it is an essential micronutrient in preventing the dental caries and for the mineralization of hard tissues. Water for domestic purpose is to be examined for its quality to identify problem parameters. If these parameters in water source exceeds the permissive limits, that source is not advisable for domestic purpose unless it is properly treated. Therefore, it is essential to perform water quality assessment of all the water sources before they are decided for domestic use. Defluoridation of drinking water is presently a common practice worldwide.

The optimum fluoride level in drinking water for general good health set by WHO is considered to be between 0.5 and 1.0 mg/l. Concentration higher than this can lead to fluorosis. Fluorosis is caused by an excess ingestion of fluoride and has caused a serious health problem for the population. Severe forms of the disease typically develop only when the F^- concentration of drinking water is greater than 5–10 mg/l. Children metabolize a higher percentage of ingested F^- than adults and are therefore particularly susceptible to fluorosis. Several methods were developed to remove fluoride and improve the quality of drinking water [1,2]. Recently, an alternative fluorite-precipitation technique using a limestone reactor have been proposed [3]. These methods are not suitable because reduction of F^- by these techniques is only upto 2 mg/l [4]. Recently other defluoridation techniques based on electrolysis and membrane processes [5] has also been studied. In recent years, much efforts have been devoted to the investigation and development of other more cost-effective F^- sorbents, such as fly ash [6], silica gel [7], bone char [8], spent catalyst [9], zeolites [10] and bentonite [11]. The fluoride adsorption by an activated alumina (AA) column seems to be an interesting process compared to other techniques. It has got good affinity and selectivity for fluoride removal.

The aim of this study was to investigate the regeneration of the AA bed saturated by fluoride ions. The performance of AA was tested under various experimental conditions. The effect of sorption parameters such as pH, initial F^- concentration, volumetric flow rates and adsorbent dose were investigated over a chosen grade of AA for repeated regeneration/reactivation cycles. Limited regeneration methods of AA column saturated by fluoride ions have been reported in the literature [12]. These techniques denote that caustic soda

Abbreviations: F^-, fluoride ion; AA, activated alumina

* Corresponding author. Tel.: +91-11-6596172; fax: +91-11-6581120.
E-mail address: kkpant@chemical.iitd.ernet.in (K.K. Pant).

1385-8947/$ – see front matter © 2003 Published by Elsevier B.V.
doi:10.1016/j.cej.2003.07.003

Nomenclature

a_p	pellet radius, m
b	Langmuir isotherm constant, 1/mg
C_b	adsorbate concentration in the bulk fluid, kg mol/m^3
C_{bo}	initial value of C_b, kg mol/m^3
C_e	equilibrium concentration, mg/l
C_o	inlet fluoride ion concentration, mg/l
C_t	outlet fluoride concentration, mg/l
D_L	axial dispersion coefficient, m^2/s
F_o	flow rate, ml/min
k, n	Freundlich isotherm constant
k_f	mass transfer coefficient, m/s
N_{Re}	Reynolds number
N_{Sc}	Schmidt number
q	amount of F^- adsorbed per unit weight of AA, mg/g AA
q_e	equilibrium adsorption capacity, mg/g AA
q_o	Langmuir constant related to the capacity and energy of adsorption, mg/g
t	flow time, s
V	interstitial velocity, m/s
V_0	value of V at inlet, m/s

Greek letters

ε	bed porosity
ρ	density, kg/m^3

Subscripts

a	ambient
i	component i
l	bulk fluid
s	solid (adsorbent) phase

was more efficient than other chemicals such as aluminium sulfate, sulfuric acid and aluminates. The performance of the regeneration operations were tested with synthetic fluorinated water. Another objective was to correlate the experimental breakthrough curves with the predicted model.

1.1. Principle of defluoridation and regeneration

Removal of fluoride by AA is mainly due to the ion-exchange and can be described by following equations:

$$\overline{{}^*\mathrm{AlOH}} + \mathrm{F^-} \Leftrightarrow \overline{{}^*\mathrm{AlF}} + \mathrm{OH^-} \quad (1)$$

$$\overline{{}^*\mathrm{AlOH_2{}^+}} + \mathrm{F^-} \Leftrightarrow \overline{{}^*\mathrm{AlF}} + \mathrm{H_2O} \quad (2)$$

$$\overline{{}^*\mathrm{AlOH}} + 2\mathrm{F^-} \Leftrightarrow \overline{{}^*\mathrm{AlF_2{}^-}} + \mathrm{OH^-} \quad (3)$$

Eq. (3) is valid at very high concentration of fluoride loading per unit weight of AA. Al represents alumina surface and the over bar denotes the solid phase.

The following reactions take place in adsorption regeneration/reactivation cycle:

$$\overline{{}^*\mathrm{AlF}} + \mathrm{OH^-} \Rightarrow \overline{{}^*\mathrm{AlOH}} + \mathrm{F^-} \quad (4)$$

$$\overline{{}^*\mathrm{AlOH}} + \mathrm{H_2SO_4} \Rightarrow \overline{{}^*\mathrm{AlHSO_4}} + \mathrm{HOH} \quad (5)$$

Eq. (5) represents the treatment with sulfuric acid for activation of adsorbent.

2. Materials and methods

2.1. Experimental

The adsorbent used was AA, supplied by Oxide India Ltd., Durgapur, Grade OA-25. The properties of the AA are given in Table 1. Synthetic water was used in this study, which was prepared by adding appropriate quantity of sodium fluoride (NaF) to distilled water to give fluoride in the required concentration range. The quantitative analysis of the fluoride ions in the sample was done using SPADNS photometric method. Our study involved the single component continuous fixed-bed adsorption of fluoride.

In the first step, the optimization of the process was achieved under various experimental conditions. The experiments were performed in batch and continuous operation. Batch adsorption experiments were carried out by taking adsorbent (AA) in the range of 4–40 g/l of synthetic fluoride samples of known concentration (2.5–14 mg/l) in different conical glass flasks. The samples were placed in a shaking thermostat with a constant speed of 70 rpm. For each set of experiment, agitation was carried out till equilibrium was reached. At different time intervals, samples were collected and the F-concentration was determined using SPADNS photometric method. For column experiments, a Perspex column (i.d. 50.8 mm, length 550 mm) was used with a feed reservoir of 20 l capacity at the top of the column. The inlet flow rate was controlled by a flow controller. At the bottom of the column, there was an orifice of 2 mm diameter

Table 1
Properties of AA, Grade OA-25 (Oxide India Ltd.)

S.no.	Characteristics	Value
1	Particle form	Spheres
2	Particle size, mm	2–5
3	Water adsorption capacity at 30 °C by wt.%	21
4	Surface area, m^2/g (minimum)	250
5	Pore volume, cm^3/g	0.42
6	Bulk density, g/cm^3	0.800
7	Bed crushing strength, wt.% (minimum)	92
8	Loss on attrition, wt.% (maximum)	0.3
9	Loss on ignition (250–1000 °C) (%)	7.5
	Chemical analysis	
10	Al_2O_3 (by difference) (minimum)	92.0
11	Fe_2O_3 (maximum)	0.05
12	SiO_2 (maximum)	0.20
13	Na_2O (maximum)	0.30

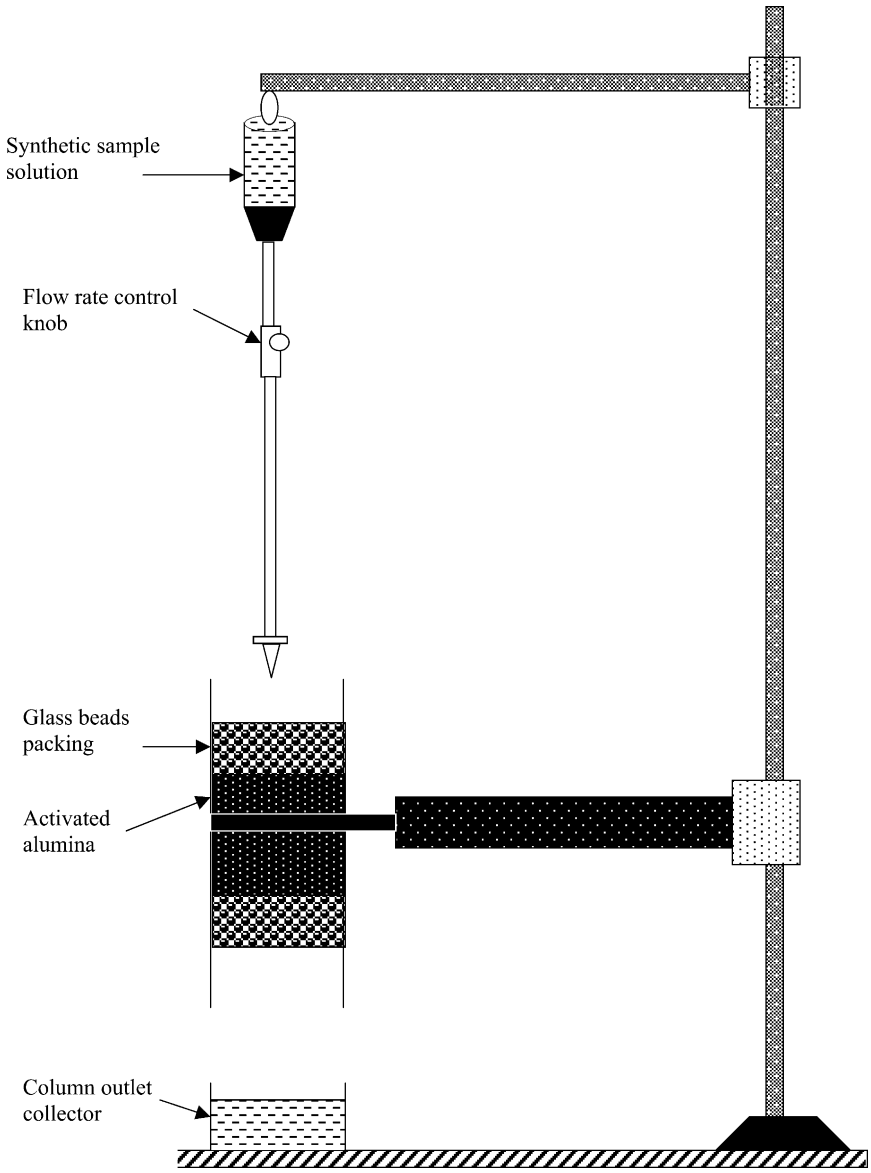

Fig. 1. Schematic diagram of experimental setup for Column Study.

from which the effluent was collected in the lower bucket at different interval of time. For the uniform distribution of liquid, glass beads were placed above the adsorbent. The schematic experimental setup for the column experiments is shown in Fig. 1.

2.2. Column studies

Column operations are essential for industrial scale designing of the fixed-bed adsorber system. The objective of the column experiments was to study the effect of process parameters such as raw water, inlet flow rate, initial fluoride concentration and bed height at various throughput volumes. Runs were made at different flow rates and at various initial concentrations to study the change in the uptake capacity of F^-. Samples of the outlet bulk solution were collected at a fixed time interval and examined for the F^- concentration. Exhausted AA bed was regenerated in situ in column using acid/alkali treatment. Any innovative technique that can reduce the cost of regeneration operation will contribute in making adsorption more efficient and more attractive. Regenerant used for exhausted AA regeneration/reactivation included NaOH and H_2SO_4 either separately or in combination. Exhausted AA was dipped in 0.1N NaOH and then left for 12 h. Then, the adsorbent, AA was washed repeatedly with distilled water and then transferred to a flask containing 0.4N H_2SO_4 solution and left overnight for activation. Subsequent water washing was carried to raise the pH to 7 followed by drying in oven for 2 h. This makes AA ready for the next defluoridation cycle. The procedure was used for the regeneration of exhausted AA after each cycle and continued upto three to five cycles in order to

study the effect of various parameters on fluoride uptake capacity.

3. Results and discussion

3.1. Batch studies

3.1.1. Equilibrium studies

In order to determine the adsorption capacity of F^-, isotherms were attempted by analyzing adsorption data to fit Freundlich and Langmuir isotherms. The Freundlich model, which is an indicative of surface heterogeneity of the sorbent, was used to explain the observed phenomena. The equilibrium data were analyzed using, the following linearized equation:

$$\log q_e = \log k + \frac{1}{n}\log C_e \quad (6)$$

where k and $1/n$ are Freundlich constants related to adsorption capacity and adsorption intensity, respectively. The value of k is 1.78 mg/g and $1/n$ is 0.32 for Freundlich isotherm. Since the value of the constant, $1/n$ (adsorption intensity) is less than unity, it indicates a favorable adsorption [13]. The Langmuir equation which is valid for monolayer sorption onto a surface with a finite number of identical sites is given by:

$$\frac{1}{q_e} = \frac{1}{q_o b}\left(\frac{1}{C_e}\right) + \frac{1}{q_o} \quad (7)$$

where q_o is the maximum amount of the F-ion per unit weight of AA to form a complete monolayer on the surface bound at high C_e, and b is a constant related to the affinity of the binding sites. q_o represents a practical limiting adsorption capacity when the surface is fully covered with metal ions and assists in the comparison of adsorption performance, particularly in case where the sorbent did not reach its full saturation in experiments. The values of Langmuir parameters, q_o and b are 0.74 mg/g and 0.31 l/mg, respectively.

3.1.2. Effect of pH

To study the effect of pH, experiments were carried out by taking the F^- spiked sample of initial concentration of

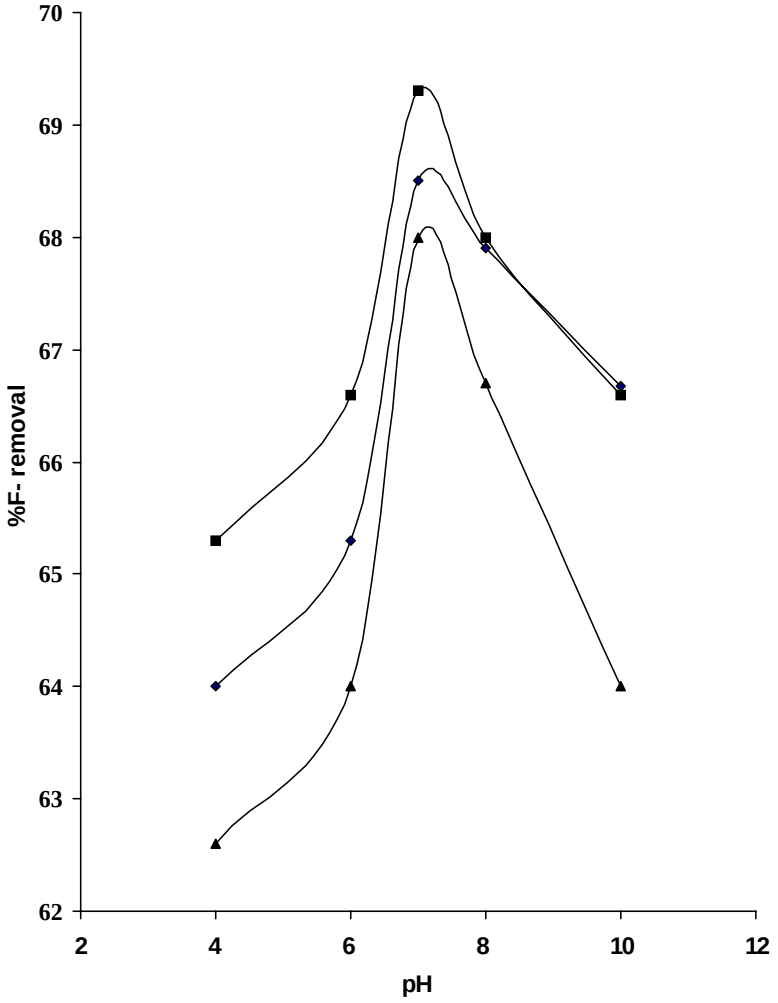

Fig. 2. Effect of pH (Batch Study) on removal of fluoride: (■) first regeneration cycle; (◆) second regeneration cycle; (▲) third regeneration cycle.

13.8 mg/l with AA dose of 4 g/l and in the pH range of 4–10. It is apparent from Fig. 2 that percentage fluoride removal increased in the solution for pH range from 4 to 7. Further increasing the solution pH from 7 to 8 and then to 10, the percent removal decreased. Results showed that adsorption reached a maximum at normal water pH of 7. In their study, Hao and Huang [12] reported that at pH > 7, silicates and hydroxyl ions appeared to compete more strongly with F^- ions for alumina exchange sites. At pH < 7, the soluble alumino–-fluoro complexes are formed resulting in the presence of aluminium ions in the treated water. Hence, it is preferable to carry out defluoridation at normal water pH to avoid aluminium dissolution and moreover no acid/alkali treatment is required after treatment. In case of Grade OA-25 of AA, maximum uptake of 1450 mg/kg AA was obtained at pH 7. Effect of regeneration has also been shown in Fig. 2. The maximum regeneration efficiency of 96% was obtained for a pH of 7. There was a reduction in uptake capacity after each regeneration cycle. The data showed that regenerated AA has the affinity towards adsorption of F^- ions.

3.2. Column studies

3.2.1. Analysis of experimental data

Initially, most of the fluoride ions were adsorbed, hence the solute concentration in the effluent was low. As adsorption continues, the effluent concentration rises, slowly at first but then abruptly. The general position of the breakthrough curve along the volume axis depends on the capacity of the column with respect to the feed concentration, flow rate and bed height. Removal of fluoride ion with flow volume can also be found from the ratio of adsorbed quantities to the amount of fluoride ion sent to the column. The total quantity sorbed in the column for a given feed concentration is equal to the area under the breakthrough curve obtained from the plot of adsorbed concentration versus effluent volume. The design of a fixed-bed adsorber and prediction of the length

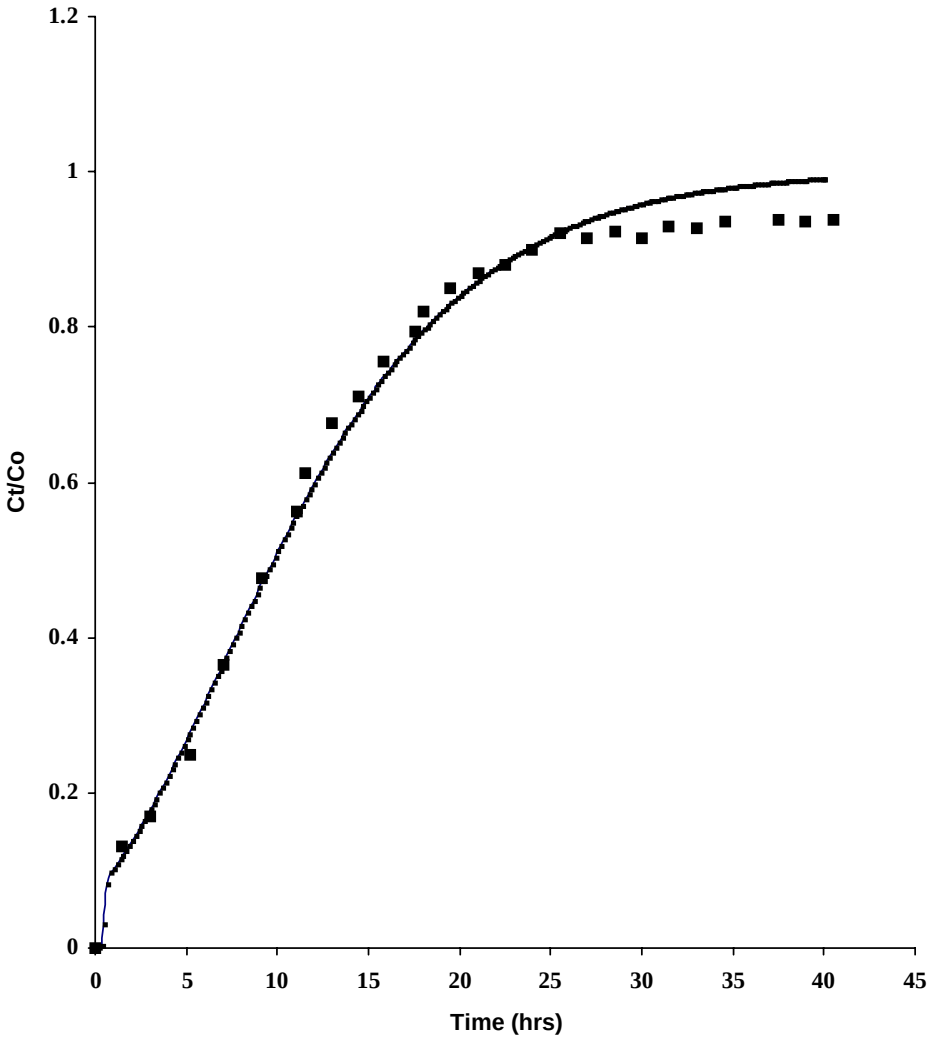

Fig. 3. Comparison of experimental breakthrough curve with theoretical ($C_o = 5$ mg/l, $F_o = 30$ ml/min); (▪▪▪) theoretical; (■) experimental.

of the adsorption cycle between regeneration require knowledge of the approach to saturation at the breakpoint.

3.2.2. Breakthrough studies

The characteristic shape of the breakthrough curve depends on the inlet flow rates, concentration and other properties such as column diameter, bed height, etc. [14–16]. The fixed-bed of certain dimensions has a definite capacity to adsorb the solute entering the bed which is equivalent to saying that the adsorbent packed in the bed would remove pollutant not only until that time when an equilibrium relationship is attained but also upon the transfer mechanism and upon the rate of adsorption [16]. The sharpness of the curve indicates not only that the system displays a linear or non-linear equilibrium isotherm but also a rate process proportional to the solute concentration in that phase which is controlling the mass transfers operation. In present study, the shape of the curve shows that adsorption is mainly mass transfer controlling. A mathematical study of breakthrough analysis was done using a one-dimensional model for isothermal, non-equilibrium, non-adiabatic, axially dispersed single component fixed-bed adsorption [17].

For the control volume, dz, for a limiting situation $z \to 0$, net rate of accumulation or depletion is given as:

$$\frac{\partial C_{bi}}{\partial t} = D_{Li}\frac{\partial^2 C_{bi}}{\partial z^2} - V\frac{\partial C_{bi}}{\partial z} - C_{bi}\frac{\partial V}{\partial z} - \frac{(1-\varepsilon)}{\varepsilon}\rho_s\frac{\partial q_{pi}}{\partial t} \tag{8}$$

The axial dispersion coefficient, D_L is calculated from the correlation:

$$D_L\left(\gamma_1 + \frac{\gamma_2 d_p \nu}{D}\right)$$

where $\gamma_1 = 0.45 + 0.55\varepsilon$ and $\gamma_2 = 0.5(1+(13\gamma_1\varepsilon/(Re \times Sc)))^{-1}$.

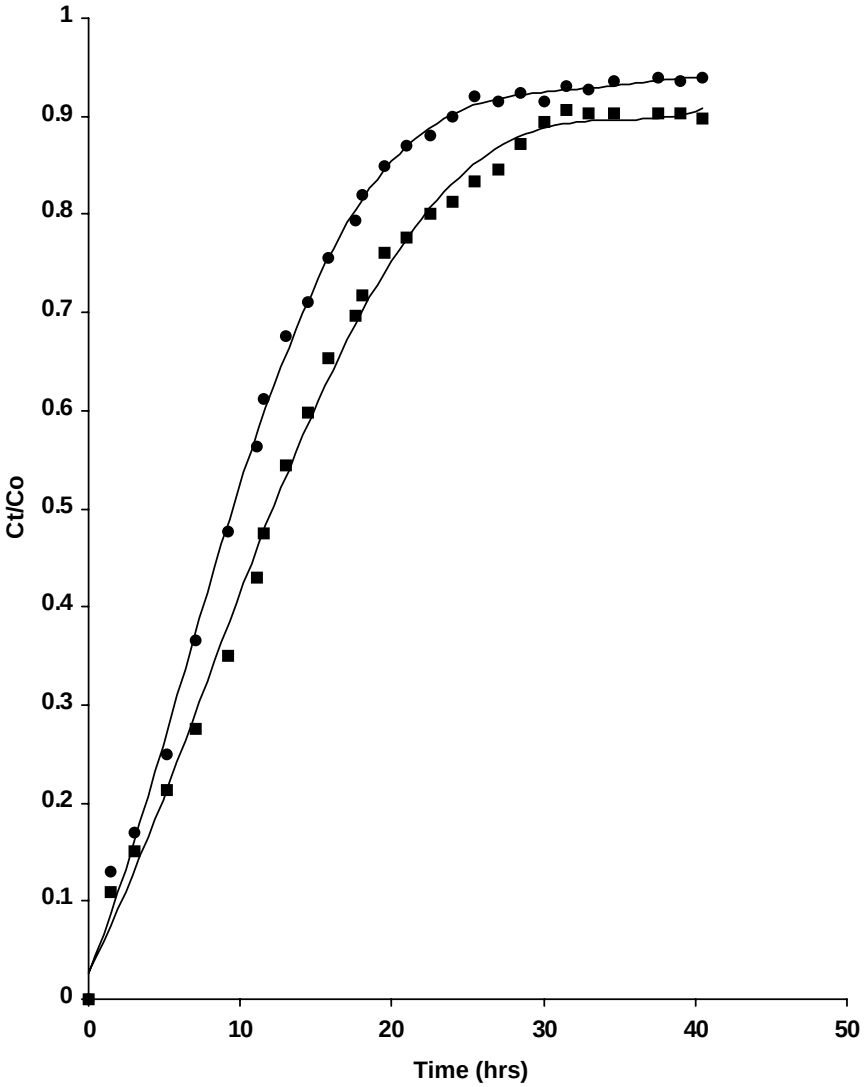

Fig. 4. Effect of flow rate on fluoride removal at $C_o = 5$ mg/l (Column Study), (●) $F_o = 30$ ml/min; (■) $F_o = 20$ ml/min.

The initial and the boundary conditions were:

$$C_{bi} = C_{bio}, \qquad z = 0,\ t = 0$$
$$D_{Li}\frac{\partial C_{bi}}{\partial z} = -V_0(C_{bio} - C_{bi}), \qquad z = 0,\ t > 0$$
$$\frac{\partial C_{bi}}{\partial z} = 0, \qquad z = L,\ t \geq 0$$

The superficial velocity, V in fixed-bed adsorption was not constant because of adsorption. The following equation was used to estimate (dV/dz), the variation of velocity of bulk fluid along the axial direction of the bed. For liquid adsorption, assuming the liquid density to be constant, then the total mass balance gives:

$$\rho_l\frac{\partial V}{\partial z} = -(1-\varepsilon)\rho_s\frac{\partial q_p}{\partial t} \tag{9}$$

Velocity boundary conditions:

$$V = V_0, \quad z = 0,\ t > 0$$
$$\frac{\partial V}{\partial t} = 0, \quad z = L,\ t > 0$$

The inter-phase mass transfer rate may be expressed as:

$$\rho_s\frac{\partial q_{pi}}{\partial t} = \frac{3k_{fi}}{a_p}(C_{bi} - C_{si}) \tag{10}$$

The magnitude of k_{fi}, depends upon the flow condition around the pellet. The following correlation was used for estimating the external mass transfer coefficient, k_f [18]:

$$Sh = 1.85\left(\frac{1-\varepsilon}{\varepsilon}\right)^{0.33}(Re^{0.33} \times Sc^{0.33}),$$
this relation is valid for $Re < 40$ (11)

The intra-pellet mass transfer is due to the diffusion of adsorbate molecules through the pore. The macroscopic conservation equation is given as:

$$\varepsilon_p\frac{\partial C_i}{\partial t} + (1-\varepsilon_p)\frac{\partial q_{ci}}{\partial t} = D_{pi}\left(\frac{\partial^2 C_i}{\partial r^2} + \frac{1}{r}\frac{\partial C_i}{\partial r}\right) \tag{12}$$

With initial and boundary conditions:

$$C_i = 0,\ q_{ci} = 0, \qquad 0 < r < a_p,\ t = 0$$
$$\frac{\partial C_i}{\partial r} = 0, \qquad r = 0,\ t > 0$$
$$k_{fi}(C_{bi} - C_{si}) = D_{pi}\frac{\partial C_i}{\partial r}, \quad r = a_p,\ t > 0$$

These equations were solved numerically using backward implicit method.

Backward implicit scheme: solving Eq. (8), we get:

$$C_{bik-1,n+1}\left[\frac{D_{Li}\Delta t}{\Delta z^2} + \frac{V_k\Delta t}{2\Delta z}\right] - C_{bik,n+1}\left[1 + \frac{2D_{Li}\Delta t}{\Delta z^2} + \frac{\Delta t}{\Delta z}(V_k - V_{k-1}) + \left(\frac{1-\varepsilon}{\varepsilon}\right)\frac{3k_{fi}\Delta t}{a_p}\right]$$
$$+ C_{bik+1,n+1}\left[\frac{D_{Li}\Delta t}{\Delta z^2} + \frac{V_k\Delta t}{2\Delta z}\right] = -\left(\frac{1-\varepsilon}{\varepsilon}\right)\frac{3k_{fi}\Delta t}{a_p}C_{sik} - C_{bik,n} \tag{13}$$

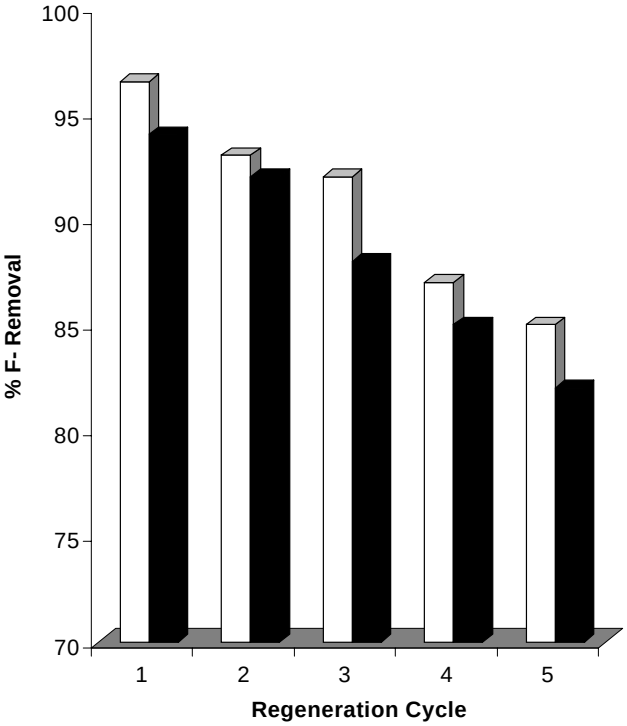

Fig. 5. Effect of initial concentration of fluoride on percent adsorption at $F_o = 20$ ml/min (Column Study), (□) $C_o = 2.8$ mg/l; (■) $C_o = 5$ mg/l.

At $t > 0$,

$$\left(1 + \frac{V_0\Delta z}{D_{Li}}\right)C_{bk,n+1} - C_{bk+1,n+1} = \frac{V_0\Delta z}{D_{Li}}C_{bi,in}, \quad z = 0$$

$$x_1C_{bk,n+1} - C_{bk+1,n+1} = x_2C_{bio}$$
$$C_{bik,n+1} - C_{bik-1,n+1} = 0, \quad z = L$$
$$x_3C_{bik-1,n+1} - x_4C_{bik,n+1} + x_5C_{bik+1,n+1} = x_6$$

The axial velocity gradient (Eq. (9)) was discretized into finite difference form as:

$$V_k = V_{k-1} - \frac{3(1-\varepsilon)M_ak_fi\Delta z}{\rho_l\varepsilon a_p}(C_{bi,k} - C_{is,k}) \tag{14}$$

Intra-pellet mass transfer (Eq. (12)) is discretized to give:

$$C_{ij-1,n+1}\left[\frac{D_{pi}}{\Delta r^2} - \frac{D_{pi}}{2(j-1)\Delta r}\right] - C_{ij,n+1}\left[\frac{\varepsilon_p}{\Delta t} + \frac{2D_{pi}}{\Delta r^2}\right]$$
$$+ C_{ij,n+1}\left[\frac{D_{pi}}{\Delta r^2} + \frac{D_{pi}}{2(j-1)\Delta r}\right]$$
$$= \left(\frac{\varepsilon_p}{\Delta t}\right)C_{ij,n} + \left(\frac{1-\varepsilon_p}{\Delta t}\right)(q_{ij,n+1} - q_{ij,n}) \tag{15}$$

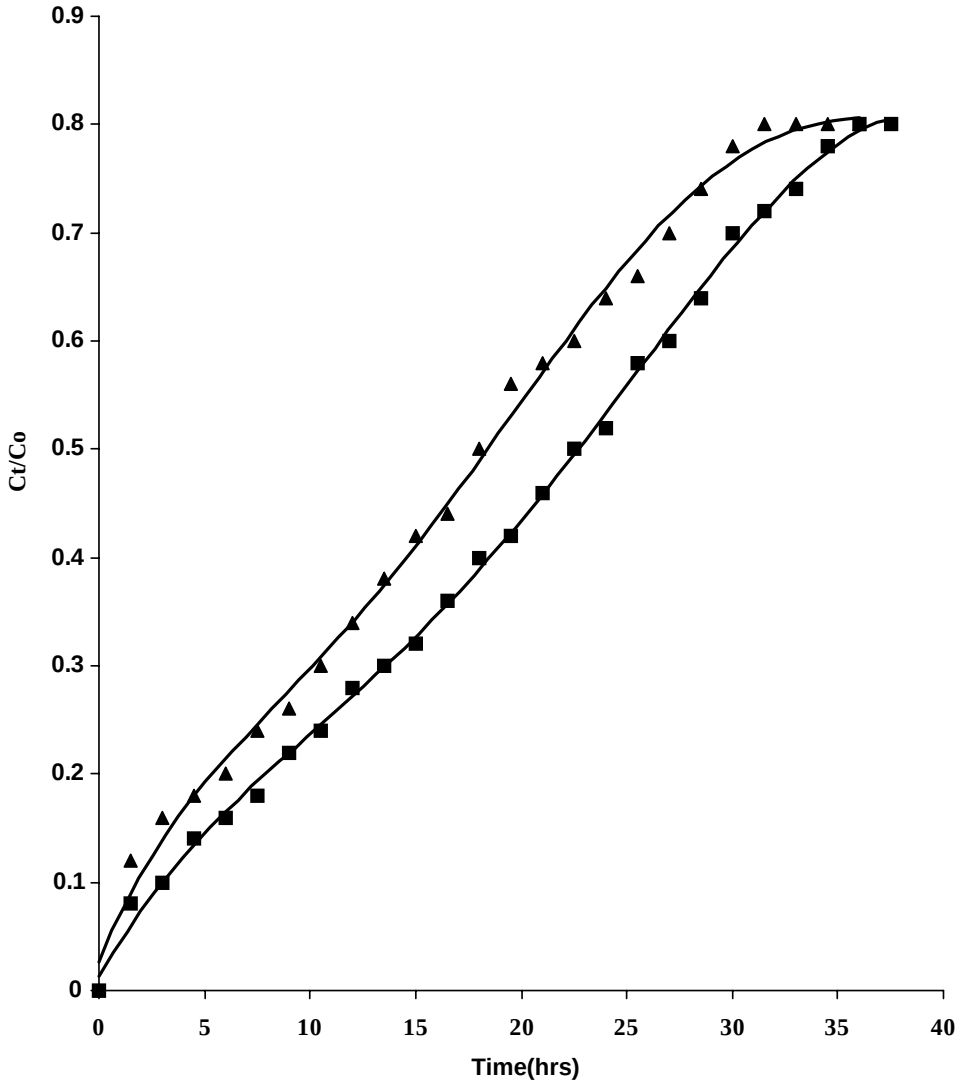

Fig. 6. Effect of bed height at $C_o = 5$ mg/l (Column Study), (▲) bed height = 5 cm; (■) bed height = 10 cm.

Initial and boundary conditions can be written as:

$$\text{At } t = 0, \quad C_i = q_i = 0, \qquad 0 < r < a_p$$
$$\text{At } t > 0, \quad C_{ij,n+1} - C_{ij+1,n+1} = 0, \quad r = 0,$$

$$\left(1 + \frac{k_{fi}\Delta r}{D_{pi}}\right) C_{ij+1,n+1} - C_{ij,n+1} = \left(\frac{k_{fi}\Delta r}{D_{pi}}\right) C_{bik,n+1}, \quad r = a_p \tag{16}$$

The above equations were solved to obtain the bulk concentration and concentration in pore fluid at various radial and axial positions. The simulated breakthrough curves for fluoride removal were optimized for a different value of mass transfer coefficient to match with the experimental data. A typical breakthrough curve is shown in Fig. 3. The values of mass transfer coefficient and axial dispersion coefficient were 5.6×10^{-5} m/s and 5.9×10^{-10} m^2/s, respectively.

3.2.3. Effect of flow rate

The effect of flow rate and inlet F^- concentration for adsorption on AA were investigated in a packed-bed column. In the first stage, the effect of flow rate was studied at 20 and 30 ml/min, while the inlet fluoride concentration in each experiment was kept constant at 5 mg/l. At a lower flow rate of 20 ml/min, the adsorption with time was very efficient in the initial step of process. This fact is probably associated with the availability of reaction sites able to capture metal ions around or inside the cells. In the second stage, with the gradual occupancy of these sites, the uptake becomes less effective. Even after breakthrough occurs the column is still capable of accumulating fluoride although at a progressively lower efficiency.

As the flow rate increased, the breakthrough curve becomes steeper. The break point time and adsorbed ion concentration decreases. The reason for this behavior can be explained in the following way: if the residence time of the solute in the column is not long enough for adsorption equilibrium to be reached at that flow rate, the fluoride solution leaves the column before equilibrium occurs. Thus, at higher flow rate the contact time of fluoride ions with AA is very short, causing a reduction in removal efficiency. Breakthrough curves, C_t/C_o versus throughput is shown in Fig. 4 for two different flow rates, 20 and 30 ml/min. The maximum percent fluoride removals for these two flow rates were found to be 92 and 86%, respectively. Regeneration/reactivation of exhausted AA bed were carried out for repeated cycles. There is a loss of 2 and 5% in the uptake capacity of AA after five cycles of regeneration for 30 and 20 ml/min, respectively.

3.2.4. Effect of initial fluoride concentration

Removal of fluoride with respect to volume of flow past the column at different flow rates and different initial concentrations of 2.8 and 5 mg/l for various regeneration cycles are shown in Fig. 5. Fluoride adsorbed by AA in the packed column depends on the volume of flow passed. The effluent volume shows whether fluoride uptake by AA is subjected to saturation limits. Sharper breakthrough curves were obtained with AA at 5 mg/l of inlet fluoride concentration and at all flow rates. At lower flow rate relatively higher uptake was observed for adsorption at the beginning of operation due to the magnitude of the concentration driving force. As solution continues to flow, the concentration of fluoride in the effluent rapidly increases. Finally the bed becomes saturated with fluoride and the concentration of solute in the effluent rises to the inlet fluoride concentration. The fluoride removal was 88 and 97% for a concentration of 5 and 2.8 mg/l, respectively. Regeneration of AA bed was carried for five cycles. A loss of 5% in uptake capacity of AA was observed during the regeneration operation after five cycles.

3.2.5. Effect of bed height

To study the effect of bed height on fluoride removal sorbent dose, 100 and 200 g was placed in the column. Fluoride spiked distilled water ($C_o = 2.8$ and 5 mg/l) was passed through the column till the treated fluoride concentration reached 1 mg/l. The typical characteristic curves are shown in Fig. 6. As can be seen from Fig. 6, an increase in the bed height from 5 to 10 cm (corresponding AA doses of 100 and 200 g), for corresponding AA doses of 100 and 200 g, respectively, the breakthrough curve becomes gentler. Thus, it is recommended to operate the unit at a minimum contact of 5 min when the bed depth is 10 cm. A similar results have also been reported on Alkoa F1 [2], where a minimum of 5 min contact time was be given for fluoride removal.

4. Conclusions

Following points can be summarized from the above studies:

(1) AA (Grade OA-25) has shown promising results for the removal of fluoride from drinking water. An adsorption capacity of 1450 mg/kg was obtained at pH 7.
(2) The breakthrough curves for adsorption of fluoride from dilute solutions using AA show the mutual effects of the adsorption capacities and adsorption rate and can explain the dependence of the shape of the breakthrough curves on experimental parameters.
(3) The adsorption capacity is strongly dependent on the flow rate, inlet fluoride ion, and bed height and is greater under conditions of high contact time, lower concentration of fluoride.
(4) As the flow rate increased, the breakthrough curve became steeper, the break point time and adsorbed ion concentration decreased. Much sharper breakthrough curves were obtained with AA at higher inlet fluoride concentration.
(5) In the regeneration studies, the uptake capacity of AA decreased after every cycle of operation. Regeneration procedure resulted in 85% efficiency with the grade of AA studied. A loss of 5% in uptake capacity of AA was observed after five cycles.

References

[1] H. Lounici, L. Adour, D. Belhocine, A. Elmidaoni, B. Barion, N. Mameri, Desalination 114 (1997) 241.
[2] F.J. Rubel, R.D. Woosely, J. Am. Water Works Assoc. 145 (1979) 45.
[3] E.J. Reardon, Y. Wang, Environ. Sci. Tech. 24 (2000) 3247.
[4] Y. Wang, J.E. Reardon, Appl. Geochem. 16 (2001) 531.
[5] H. Lounici, L. Adour, D. Belhocine, A. Elmidaoni, B. Barion, N. Mameri, Chem. Eng. J. 81 (2000) 153.
[6] A.K. Chaturvedi, K.P. Yadava, K.C. Pathak, V.N. Singh, Water Air Soil Pollut. 49 (1990) 51.
[7] R. Wang, H. Li, Y. Wang, Water Qual. Res. J. Can. 30 (1995) 81.
[8] D.S. Bhargava, D.J. Killedar, Water Res. 26 (1992) 781.
[9] Y.D. Lai, J.C. Liu, Sep. Sci. Tech. 31 (1996) 2791.
[10] S. Mayadevi, Ind. Chem. Eng. A 38 (1996) 155.
[11] M. Simurali, A. Pragathi, J. Karthikeyan, Environ. Pollut. 99 (1998) 85.
[12] O.J. Hao, C.P. Huang, J. Environ. Eng. Div. ASCE 112 (1986) 1054.
[13] M. Prasad, S. Saxena, S.S. Amritphale, N. Chandra, Ind. Chem. Eng. 42 (2000) 170.
[14] Z. Aksu, D. Ozer, A. Ozer, T. Kutsal, C. Arif, Sep. Sci. Tech. 33 (1998) 667.
[15] C. Gabaldon, P. Marzal, A. Seco, J.A. Gonzalez, Sep. Sci. Tech. 35 (2000) 1039.
[16] H. Mohanmadinejad, J.C. Knox, J.E. Smith, Sep. Sci. Tech. 35 (2000) 1.
[17] W. Jin, S. Zhu, Chem. Eng. Tech. 23 (2000) 151.
[18] T. Kataka, H. Yoshida, K. Ueyama, J. Chem. Eng. Jpn. 5 (1972) 132.